SCICELL

Nova Biotechnol Chim (2020) 19(1): 98-108
DOI: 10.36547/nbc.v19i1.582

Nova Biotechnologica *et* Chimica

Factors affecting the analysis of 2-deoxy-2-fluoro[^{18}F]-D-glucose in plant tissues by a commercial PET system

Vanda Adamcová[1], Klára Kuglerová[1], Katarína Ondreičková[2], Marcela Gubišová[2], Jozef Gubiš[2], Juraj Lesný[1], Peter Kováč[1,3] and Miroslav Horník[1,✉]

[1]*Department of Ecochemistry and Radioecology, Faculty of Natural Sciences, University of SS. Cyril and Methodius in Trnava, Nám. J. Herdu 2, Trnava, SK-917 01, Slovak Republic*

[2]*National Agricultural and Food Centre – Research Institute of Plant Production, Bratislavská cesta 122, Piešťany, SK-921 68, Slovak Republic*

[3]*BIONT Inc., Karloveská 63, Bratislava, SK-842 29, Slovak Republic*

Article info

Article history:
Received: 15th May 2020
Accepted: 10th June 2020

Keywords:
2-[^{18}F]FDG
PET
Plant tissues
Uptake
Quantification
3D imaging

Abstract

Some works showed that commercial PET systems and 2-deoxy-2-fluoro[^{18}F]-D-glucose (2-[^{18}F]FDG) can be used in plant studies to analyze the transport and allocation of photoassimilates. The aim of this work was to evaluate the effect of characteristics of plant tissues, applied solution and of the phenomenon of "escaping positrons" on the visualisation and quantification of the distribution of 2-[^{18}F]FDG, as a model of photoassimilates, in the tissues of selected plants by a commercial PET system. Experiments included pepper plants immersed with the root system or stem into a 2-[^{18}F]FDG solution showed that the accumulation of 2-[^{18}F]FDG was several times higher in the aboveground parts that were not directly exposed in a 2-[^{18}F]FDG solution than in the parts directly immersed in the solution. Individual experiments carried out by exposing the excised leaves of radish plants in the solutions of 2-[^{18}F]FDG containing 100-fold higher concentrations D-glucose (c_{glu}) compared to the original 2-[^{18}F]FDG solution showed that with increasing c_{glu} there were significant changes in the distribution of 2-[^{18}F]FDG in the leaf blade. The last factor studied was the phenomenon known as "escaping positrons" and defined by annihilation of released positrons during radioactive decay of a given emitter ^{18}F outside the studied object, whose thickness exceeds the lower limits of resolution of PET systems It was found that the covering the leaf of tobacco, after exposure in a 2-[^{18}F]FDG solution, by a parafilm, aluminium foil or copper thin plate caused significant changes in the quantitative data obtained in the PET analysis.

Introduction

Rapidly growing human population increases requirements on food, energy and other natural resources. Advances in molecular biology techniques developed crops that are more resistant to pathogen microorganisms, viruses, insects and abiotic stress, such as temperature, nutrient limitation, etc. and they are widely available to improve food and energy production (Wang *et al.* 2014).

Soil provides most of the essential elements required for the growth of plants. These elements are absorbed by the root system and then are transported into the leaves *via* the xylem and photoassimilates and other nutrients are translocated from the leaves to the maturing organs *via* the phloem. For centuries, scientists have been fascinated by water and sugar

✉ *Corresponding author:* hornik@ucm.sk

transport in plants because these processes are important for plant growth and cycle. If we aspire to explain plant growth or to increase the productivity of agriculture or forestry, it is crucial to understand the dynamics and the controls of water and sugar flow, as well as their interactions. Therefore, an accurate understanding of the movement of metabolites and elements across the plant body is of paramount importance in plant science research (Suzui *et al.* 2019). It is also essential to unravel how transport in plants affects their functioning and their ability to withstand stress, and also which conditions determine whether a plant thrives or dies (Hubeau and Steppe 2015).

Research focused on the distribution and dynamics of photoassimilates in plants is important for increasing food production. Imaging methods based on radioisotopes application represent unique technics to understand the kinetics of elements and bioorganic compounds in the plant body (Suzui *et al.* 2019). Furthermore, non-invasive radioisotopes imaging techniques, which can image the temporal changes in radioisotopes distributions, are effective for investigating the dynamics and distributions of elements and molecules under *in vivo* conditions. In plant studies, they are powerful tools for the elucidation of physiological functions (Kurita *et al.* 2020). The field of radiotracer imaging involves the application of radioisotope-labelled compound (radiotracer) to analyze the uptake and distribution of corresponding non-labelled analogue, thus helping to shed light on the underlying physiology or diagnostics (Fatangare and Svatoš 2016). One of these radiotracer imaging systems and approaches is positron emission tomography (PET).

PET is a non-destructive imaging method based on the injection of radiotracer labelled with a positron-emitting radionuclide. This method represents a highly sensitive nuclear medicine technique that enable to visualize the disposition and kinetics of radioisotopes *in vivo*. The advantage of the technique lies in the wide range of available radiotracers that produce image contrast directly related to underlying physiology, metabolic pathways, or molecular targets (Berg and Cherry 2018; Moein *et al.* 2019). PET scanners consist of a cylinder of scintillation detectors coupled to fast electronics, feeding into software. The detectors collect coincident pairs of 511 keV γ-photons emitted at 180°, which originate from the site where a positron produced by radioactive decay annihilates with an electron in the surrounding material. The generated three-dimensional (3D) images map the distribution of a positron-emitting radionuclide. PET is an ultra-sensitive technique allowing the detection of very low amounts of radiotracer ($< 10^{-16}$ moles, 10 kBq) and a good spatial resolution between 1 and 6 mm, depending on the construction of the detector and the image reconstruction algorithm (Thorpe *et al.* 2019).

PET has been primarily used for clinical (human) and preclinical (animal) applications. A common use of PET in clinical practice is for the diagnosis of various cancers and in preclinical applications. PET is also often used in drug development through animal-based imaging studies. Additionally, PET has proven to be very useful particularly in plant biology research applications.

Medical imaging techniques are rapidly expanding in the field of plant science (Weisenberger *et al.* 2013; Hubeau and Steppe 2015). PET can be used to study whole-plant transport and nutrient allocation by quantifying the distribution of a positron-emitting radioisotope non-invasively, over a time-course, and with a spatial resolution of a few millimetres (Karve *et al.* 2015). The advantages of the PET systems mainly include the capability of providing dynamic images of positron-emitting isotopes under *real time* and *in vivo* conditions without damaging the plants. The commonly used positron-emitting radioisotopes include ^{18}F, ^{15}O, ^{11}C and ^{13}N, which are usually bound to bioorganic molecules to form a radiopharmaceutical targeting a particular uptake pathway. The most widely used radiopharmaceutical for imaging human is 2-deoxy-2-[^{18}F]fluoro-D-glucose (2-[^{18}F]FDG), which detect malignant tumours with faster glucose uptake than a benign tissue. The 2-[^{18}F]FDG can accumulate in any cell that has the ability to metabolise glucose, including those in subsurface anaerobic environments (Thorpe *et al.* 2019). In this glucose analogue the hydroxyl group at the C-2 position has been replaced by a ^{18}F radioisotope with a half-life $T_{1/2}$ =109.8 min (Fatangare and Svatoš 2016).

There are several works that evaluate the possibility of using commercial PET systems in visualization and quantification of uptake and transport of 2-[^{18}F]FDG in plant tissues. Tsuji *et al.* (2002)

first reported on 2-[^{18}F]FDG uptake and distribution in tomato plants. Hattori *et al*. (2008) described 2-[^{18}F]FDG translocation in intact sorghum plants and suggested its use in tracing photoassimilates translocation in plants. 2-[^{18}F]FDG has been used to study glycoside biosynthesis in plants as a measure of induction of plant response (defense) (Ferrieri *et al*. 2012). Moreover, Tran *et al.* (2017) synthetized 1′-[^{18}F]fluoro-1′-deoxysucrose and 6-[^{18}F]fluoro-6-deoxysucrose ([^{18}F]FDS) analogues and studied the role of sucrose transporter (SUT) proteins in wild-type and mutant (*sut1* mutant plants of maize (*Zea mays* L.) by phosphor imaging plate system.

In previous papers, the application potential of a commercial PET system in the characterization of the uptake and distribution of 2-deoxy-2-fluoro[^{18}F]-D-glucose labelled with the positron-emitting isotope ^{18}F (2-[^{18}F]FDG) in plant tissues of tobacco (*Nicotiana tabacum* L.) or giant reed (*Arundo donax* L.) plants was evaluated (Partelova *et al*. 2017, 2016, 2014). The aim of this work was to evaluate the effect of plant tissues characteristics, concentration of D-glucose in a 2-[^{18}F]FDG solution and the phenomenon of "escaping positrons" on the visualisation and quantification of the uptake and distribution of 2-[^{18}F]FDG in the tissues of selected plants by a commercial PET systems.

Experimental

Plant material

Plants of pepper (*Capsicum annuum* L.) and radish (*Raphanus sativus* L.) as a model of vegetables and plants of tobacco (*Nicotiana tabacum* L.) were chosen as studied objects. Seeds of pepper and radish plants were purchased as commercially available seeds (SEVA SEED, Ltd. Valtice, Czech Republic and SEMO, Inc. Smržice, Czech Republic) and seeds of tobacco plants were obtained from the Gene Bank of the Slovak Republic. Seedlings of the mentioned plant species were obtained from the seeds germinated and cultivated in an inorganic carrier Perlite watered with hydroponic medium according to Hoagland (Hoagland 1920). For these purposes, Hoagland media (HM) diluted with deionized water (0.054 μS.cm^{-1}) at a volume ratio 1 : 3 (25 % concentration strength) were used, whereby the full strength medium (100 % HM) contained macroelements (in mg.L^{-1}) $MgSO_4.7H_2O$ – 370; KNO_3 – 404; $CaCl_2$ – 444; $NaH_2PO_4.2H_2O$ – 292; $Na_2HPO_4.12H_2O$ – 46.5; $FeSO_4.7H_2O$ – 17.9; $NaNO_3$ – 340; NH_4Cl – 214; NH_4NO_3 – 160; and microelements (in mg.L^{-1}) H_3BO_3 – 8.5; $Na_2MoO_4.2H_2O$ – 0.06; $MnSO_4.5H_2O$ – 5.0; $ZnSO_4.7H_2O$ – 0.66; $CuSO_4.5H_2O$ – 0.8. The cultivation conditions – photoperiod 16 h light/8 h dark (max. photosynthetic photon flux density PPFD = 200 μmol.m^{-2}.s^{-1}), temperature max. 28 ºC (light)/min. 18 ºC (dark) and relative humidity 60 – 80 % were provided by the growth chamber for plant cultivation (KBWF 720, Binder, D). After 6 – 8 weeks of the cultivation, the uniform plants, in terms of height (approx. 15 cm), weight (approx. 1 g; w.w.), root size, number of leaves and developmental stage, were removed from the Perlite and the root system was carefully washed with tap water to remove adherent particles.

Production of 2-[^{18}F]FDG

A radioisotope ^{18}F as a positron emitter ($T_{1/2}$ = 109.5 min) in the form of F^- anions was prepared from the molecules of $H_2{}^{18}O$ *via* the reaction ^{18}O (*p, n*) ^{18}F using the cyclotron Cyclone 18/9 (IBA, Belgium). The key intermediate 1,3,4,6-tetra-*O*-acetyl-2-[^{18}F]fluoro-D-glucopyranose for the production of 2-[^{18}F]FDG was obtained from the precursor 1,3,4,6-tetra-*O*-acetyl-2-*O*-trifluoromethanesulfonyl-*β*-D-manno-pyranose and using the phase-transfer catalyst aminopolyether-potassium complex (Kryptofix® 222) and produced [^{18}F]F^- as well. Finally, 2-[^{18}F]FDG was prepared by the acid hydrolysis of mentioned intermediate. The procedures of ^{18}F production and 2-[^{18}F]FDG synthesis were realized by the company BIONT Inc. (Bratislava, Slovak Republic). The final solution of 2-[^{18}F]FDG, as a radiopharmaceutical product under the trade name biontFDG, was supplemented with NaCl (9.0 g.L^{-1}) and showed the following physico-chemical parameters (determined/evaluated by): Opalescence (organoleptically) – clear, colourless solution; pH (colorimetrically) – 6.8 – 7.2; Specific volume radioactivity (ionization chamber) – 1.6 – 2.8 GBq.mL^{-1}; Half-life decay (ionization chamber) – 109.5 min; Chemical

concentration of 2-[^{18}F]FDG (liquid chromatography) – < 0.0016 mg.mL^{-1}; Concentration of Kryptofix® 222 (thin-layer chromatography) – < 0.22 mg.mL^{-1}; Radiochemical purity of ^{18}F in the form of 2-[^{18}F]FDG and 2-deoxy-2-[^{18}F]fluoro-D-mannose (thin-layer chromatography) – 97 % – 99 %; Concentration of glucose (liquid chromatography) – 0.0762 mg.mL^{-1}; Concentration of acetonitrile (gas chromatography) – 0.03 mg.mL^{-1}; Concentration of ethanol (gas chromatography) – 0.037 mg.mL^{-1}. Before the application in the experiments, a 2-[^{18}F]FDG solution was diluted with deionised water at a volume ratio of 1 : 9.

2-[^{18}F]FDG uptake and PET analysis

The uptake of 2-[^{18}F]FDG was carried out by immersing the root system of the intact plant, the stem after the removing the root system with a scalpel, the petiole of the excised leaf or by immersing the excised apex of the leaf blade into small plastic vials containing of 2-[^{18}F]FDG solution with known volume activity of ^{18}F and D-glucose concentration. Thus, the visualization and quantification of 2-[^{18}F]FDG uptake and distribution in the tissues of selected plant parts were realized in two transport ways, in acropetal and basipetal (opposite) direction of the solute transport within the conductive tissues as well. To avoid spillage and evaporation of the water, the plastic vials were covered with a parafilm over the neck of the vial. In the case of leaf samples, the third developmentally youngest leaf branch was excised with a scalpel. The exposure was realized under laboratory conditions (temperature 23 °C – 25 °C; relative humidity 40 % – 45 %) during 30 min. After this time, the immersed plant parts were washed in deionized water by submersion, dried between cellulose towels and weighed (w.w.). Subsequently, the studied objects were carefully placed on the scanning bed of the microPET system eXplore Vista pre-clinical PET scanner (GE Healthcare, Spain) and fixed with parafilm strips so that the individual leaves did not overlap or overlap across the boundary of the tomograph bed. The acquisition of primary data was initiated using the program eXplore VISTA ver. 3.1 under conditions of a static mode during 2 min for every length of the scanning bed position (2 cm). The total number of bed positions was chosen depending on the length of the analyzed plant part.

A commercial microPET system consisted of 18 detection modules arranged in a circle with a diameter of 11.8 cm. One detection module was represented by 13 × 13 arrays of 1.45 mm × 1.45 mm × 7.0 mm lutetium oxyorthosilicate (LSO) crystals and 1.45 mm × 1.45 mm × 8.0 mm gadolinium orthosilicate single (GSO) crystals and was located in time coincidence with the seven opposite modules. This arrangement gives an effective transverse field-of-view of 6.7 cm and an axial field-of-view of 2.0 cm. The whole system provides a spatial resolution of 1.5 mm and an absolute sensitivity of the central point source of 1.9 % at the 250 – 700 keV energy window used. The control of mentioned microPET system, acquisition and reconstruction of the obtained data in the form of PET images (3D; voxel size 0.3875 mm × 0.3875 mm × 0.775 mm) were performed using the program eXplore VISTA ver. 3.1 Analysis & Visualization software that includes the mathematical algorithms 3D FORE (Fourier rebinning algorithm) / 2D OSEM (2D ordered subset expectation maximization). Within the reconstruction process, the obtained 2D sinograms were also corrected for accidental coincidences, radioactive decay and dead-time. Amide.exe ver. 1.0.4. software was used to visualize 3D PET images after their reconstruction, which allows the reduction of the maximum threshold to improve the visual quality of the regions with a lower accumulated activity.

Determination of ^{18}F activity

Gamma-spectrometric analysis was carried out to determine the residual radioactivity of 2-[^{18}F]FDG solution, as well as in the measurement of accumulated ^{18}F activity in individual parts of studied plants. For these purposes, a scintillation gamma-spectrometer with a NaI(Tl) well type crystal 54BP54/2 (Scionix, Netherlands) and ScintiVision-32 software (Ortec, USA) were used. Standard solutions of $^{109}CdCl_2$, 2-[^{18}F]FDG and ^{137}CsCl with defined activities

at a given time were applied to calibrate (γ-photon energies and measurement efficiency) of the scintillation gamma-spectrometer and a library of ^{109}Cd ($E\gamma$ = 88.04 keV), ^{18}F ($E\gamma$ = 511 keV) and ^{137}Cs ($E\gamma$ = 661.66 keV) was built. In the case of samples showing high ^{18}F activity (> 1.10^5 Bq) outside the detection limits of the scintillation gamma-spectrometric system used, these samples were analyzed by ionisation chamber Curiementor (3PTW, Germany).

Results and Discussion

Root system as a barrier for 2-[^{18}F]FDG transport

In the first part of the work, the effect of the characteristics of plant tissues on the uptake and distribution of 2-[^{18}F]FDG, as a model of photoassimilates, and on the visual and quantitative side of the PET analysis was studied. In this way, the experiments with intact pepper (*C. annuum* L.) plants immersed with the root system or cut stem into a 2-[^{18}F]FDG solution including the PET analysis using a commercial microPET primarily developed for animal objects were carried out.

It is generally known that the root system of plants acts as a natural selective barrier determining the solute transport. In this context, we focused on the comparison of the uptake and distribution of 2-[^{18}F]FDG in tissues of pepper plants after 30 min of their exposure by immersing the root system of the intact plant and the stem after the removing the root system into a 2-[^{18}F]FDG solution with known ^{18}F activity and concentration of D-glucose 7.62 mg.mL^{-1}. As can be seen from Fig. 1, for both objects analyzed, we obtained visually evaluable PET images. As was found in our previous work Partelová *et al.* (2014), the visual interpretability of PET records regarding the distribution of 2-[^{18}F]FDG in plant tissues as well as the translocation of 2-[^{18}F]FDG from the application part (root system or leaf petiole) to other parts of the plant are significantly affected by the concentration of D-glucose in the applied solution 2-[^{18}F]FDG. In the present experiments, we based these findings and therefore increased the initial concentration of D-glucose in dilute solution of 2-[^{18}F]FDG, which is applied in PET diagnostic tests, 1,000-fold to the concentration of 7.62 mg.mL^{-1}. From the obtained PET quantitative data (Table 1), it can be claimed that the accumulation of 2-[^{18}F]FDG expressed in terms of *TFc* values was several times higher in the aboveground parts that were not directly exposed in 2-[^{18}F]FDG solution than in the parts directly immersed in the solution of 2-[^{18}F]FDG. *TFc* represents coincidence transfer factor defined as the ratio of the Num_c (number of analyzed coincidences within the PET analysis) in the non-immersed parts of the plant to the Num_c in the parts of the plant immersed into a 2-[^{18}F]FDG

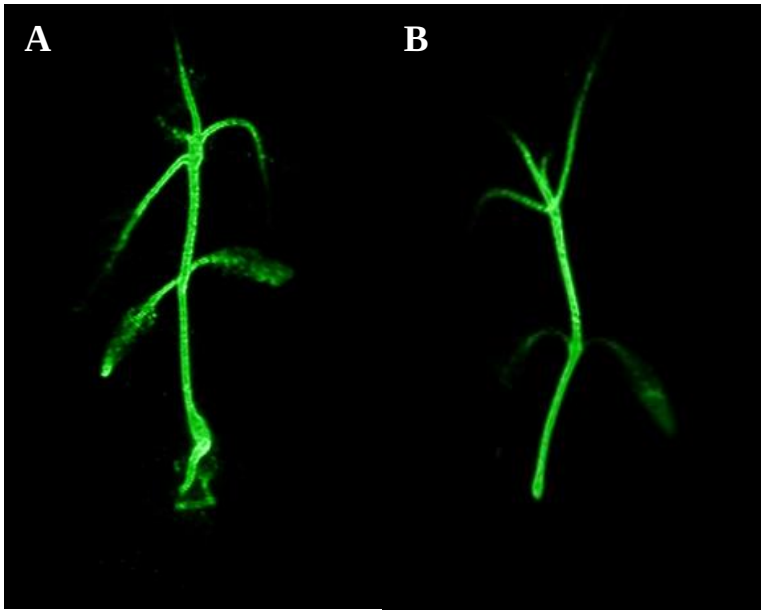

Fig. 1. Imaging of 2-[^{18}F]FDG distribution in the tissues of pepper (*C. annuum* L.) plants immersed with the root system (**A**) or cut stem (**B**) into a 2-[^{18}F]FDG solution: **A.** 100 MBq and 7.62 mg.mL^{-1} of D-glucose; **B.** 20 MBq and 7.62 mg.mL^{-1} of D-glucose. After 30 min of exposure plants were analyzed by a commercial microPET system with the acquisition time 2 min for bed position. The maximum threshold *TH* (thresholding-based methods) was reduced to 10 %.

solution. Thus, this parameter quantitatively describes the translocation of 2-[^{18}F]FDG within the evaluated plant parts. In the comparison of the analyzed pepper plants, it was found that in the case of plant immersed in a 2-[^{18}F]FDG solution with the stem after removal of the root, the *TFc* value was 2-times higher than in the case of intact pepper plant immersed in a solution of 2-[^{18}F]FDG by the root system (*TFc* = 9.4). Also, it can be concluded that there was a significantly higher translocation of 2-[^{18}F]FDG and *TFc* values compared to the values found in previous work (Partelová *et al.* 2014) in the case of tobacco plants (*N. tabacum* L.), as well as in the case of giant reed plants (*A. donax* L.) (Partelová *et al.* 2017). In the work Partelová *et al.* (2014), there were reached the values of *TFc* = 0.04 at D-glucose concentration 0.00762 mg.mL^{-1} and *TFc* = 0.21 at 0.762 mg.mL^{-1}, which indicated a significant accumulation of 2-[^{18}F]FDG in the root system and its minimal transfer to the aboveground parts of plants. Thus, it is clear that the concentration of D-glucose will play an important role in the distribution of 2-[^{18}F]FDG as a model molecule of photoassimilates within plant tissues in terms of its translocation. At the same time, it must be stated that these processes and characteristics will also depend on the study object – on the given plant species, even in the case of plants originating from the same family (family *Solanaceae*, e.g. tobacco, pepper, and tomato). These facts must be taken into account in terms of PET analysis and its relevant applicability as a non-invasive analytical method.

After the PET analysis, the pepper plants were divided into individual parts (root, stem, developmentally older and younger leaves) and analyzed for the accumulated activity of ^{18}F by direct gamma-spectrometry (Fig. 2A). Based on the obtained results, it can be concluded that in the case of a pepper plant immersed by the root system in a 2-[^{18}F]FDG solution, the accumulated ^{18}F activity decreased proportionally from the submerged root to the aboveground parts, with the lowest ^{18}F activity measured in the developmentally younger leaves. It was found that the removal of the root system resulted in increased translocation and distribution of 2-[^{18}F]FDG within the stem and accumulation of 2-[^{18}F]FDG in developmentally younger leaves in comparison with cotyledon (primary leaves), taking into account the fact of 5-fold lower applied activity of ^{18}F in the case of a pepper plant immersed with the stem into a 2-[^{18}F]FDG solution. This result was also confirmed from the point of view of percentage evaluation of the distribution of ^{18}F activity in individual parts of pepper plants of the total amount of ^{18}F activity accumulated by the plant (Fig. 2B).

Comparing the distribution of ^{18}F activity in the aboveground parts of pepper plants (Fig. 2B), the most significant difference can be observed between a plant exposed through the root system (intact plant) and a plant exposed through the stem (plant without root system), especially in the case

Table 1. Initial parameters defining the experiments and obtained quantitative data (variables) from the PET analysis of pepper (*C. annuum* L.) plants immersed with the root system or cut stem into a 2-[^{18}F]FDG solution containing 7.62 mg.mL^{-1} of D-glucose. For details, see Fig. 1.

Parameter/ Variable	Intact plant	Stem
m_P [g]	0.789	0.671
A_0 [MBq]	100	20
Num_c	4,966	3,457
TF_c	9.4	18.0
EV [cm^3]	16.73	4.35
PV	143,778	37,351
TGV	11 804,100	63 672,100
Max PV	4,557	10,228

m_P – fresh weight of the plant biomass; A_0 – initial applied activity of 2-[^{18}F]FDG solution; Num_c – number of analyzed coincidences within the PET analysis; *TFc* – coincidence transfer factor defined as the ratio of the Num_c in the non-immersed parts of the plant to the Num_c in the parts of the plant immersed into a 2-[^{18}F]FDG solution; *EV* – estimated volume within the PET analysis; *PV* – pixel volume; *TGV* – total gray value; *MaxPV* – maximum pixel value.

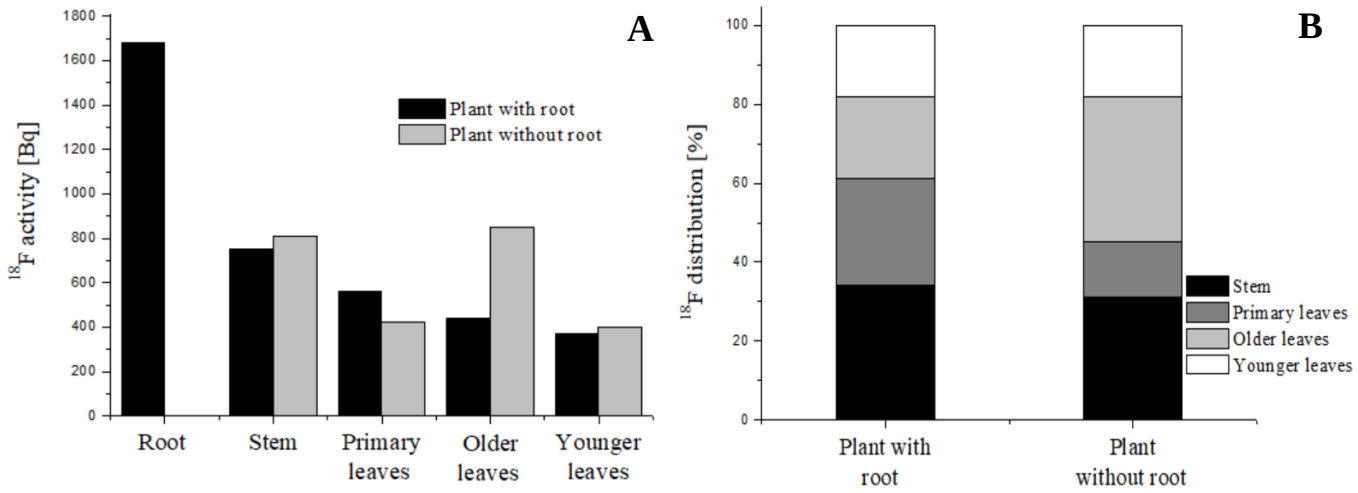

Fig. 2. A. Accumulated ^{18}F activity in the form of 2-[^{18}F]FDG within the individual parts of pepper (*C. annuum* L.) plants after their 30 min exposure by immersion of the root system or cut stem (plant without root system) into a 2-[^{18}F]FDG solution containing 7.62 mg.mL^{-1} of D-glucose. **B.** Distribution expressed in percentage of the total ^{18}F activity accumulated by the plant.

of older leaves. For the plant without root system, an increased percentage of accumulated ^{18}F activity was confirmed in developmentally older leaves (35 % of the total ^{18}F activity accumulated by the plant), while in the case of plant immersed in a solution of the 2-[^{18}F]FDG by the root system the ratio of ^{18}F activity accumulated in developmentally older leaves represents only 21 %. In the case of plant immersed in the solution of 2-[^{18}F]FDG by root system, a more significant accumulation of ^{18}F activity can be observed, especially in the stem and primary leaves, which accounted for up to 61 % of the total ^{18}F activity accumulated by the plant.

Effect of D-glucose concentration

To confirm the effect of the concentration of D-glucose (c_{glu}) in the applied solution of 2-[^{18}F]FDG on the translocation and distribution of 2-[^{18}F]FDG from the conductive tissues to parenchymal leaf blade cells, the experiments with excised leaves of radish (*R. sativus* L.) were carried out.

In the first experiment, an excised radish leaf was exposed with a petiole in the solution of 2-[^{18}F]FDG with c_{glu} = 0.00762 mg.mL^{-1} and initial ^{18}F activity A_0 = 8 MBq for 30 min under laboratory conditions. Subsequent PET analysis showed only a slight

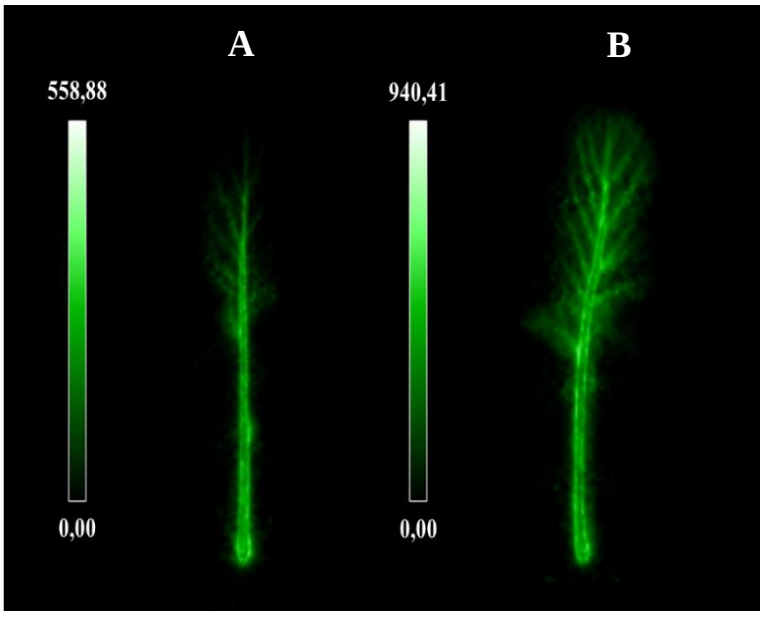

Fig. 3. Imaging of 2-[^{18}F]FDG distribution in the tissues of radish (*R. sativus* L.) leaves immersed with the petiole into a 2-[^{18}F]FDG solution: **A.** 8 MBq and 0.00762 mg.mL^{-1} of D-glucose; **B.** 8 MBq and 0.762 mg.mL^{-1} of D-glucose. After 30 min of exposure leaves were analyzed by a commercial microPET system with the acquisition time 2 min for bed position. The maximum threshold *TH* (thresholding-based methods) was reduced to 10%.

Table 2. Initial parameters defining the experiments and obtained quantitative data (variables) from the PET analysis of excised leaves of radish (*R. sativus* L.) immersed with the petiole into a 2-[^{18}F]FDG solution containing 0.00762 mg.mL^{-1} (Leaf A) or 0.762 mg.mL^{-1} (Leaf B) of D-glucose. For details, see Fig. 3.

Parameter/ Variable	Leaf A	Leaf B
m_L [g]	0.439	0.435
A_0 [MBq]	8.0	8.0
c_{glu} [mg.mL^{-1}]	0.00762	0.762
Num_c	1 235,000	2 693,000
TF_c	4.92	9.03
EV [cm^3]	3.156	4.898
PV	27,121	42,090
TGV	3 746,360	7 968,240
Max PV	5,589	9,404

m_L – fresh weight of the leaf; A_0 – initial applied activity of 2-[^{18}F]FDG solution; c_{glu} – initial concentration of D-glucose in a 2-[^{18}F]FDG solution; Num_c – number of analyzed coincidences within the PET analysis; *TFc* – coincidence transfer factor defined as the ratio of the Num_c in the non-immersed parts of the leaf to the Num_c in the parts of the leaf immersed into a 2-[^{18}F]FDG solution; *EV* – estimated volume within the PET analysis; *PV* – pixel volume; *TGV* – total gray value; *MaxPV* – maximum pixel value.

transfer of 2-[^{18}F]FDG from the major venous to the secondary veins of the radish leaf blade (Fig. 3). In contrast, in the case of PET analysis of radish leaf exposed under the same conditions as in the previous experiment, but in the solution of 2-[^{18}F]FDG with a 100-fold higher c_{glu}, obtained 3D PET record clearly indicates the increase of the translocation of 2-[^{18}F]FDG into the secondary veins of the leaf blade. The observed increase in translocation of 2-[^{18}F]FDG was also confirmed on the basis of quantitative data obtained from the PET analysis (Table 2), such as Num_c, *TGV* (total gray value) and especially *TFc*, the values of which determine and clearly correlate with the increased distribution of 2-[^{18}F]FDG within the radish leaf blade.

We suggest two hypotheses which may explain these findings. Both are associated with phloem transport of photoassimilates. The first hypothesis is related to the mechanism of sugar transport in plant conductive tissues. In plant physiology, the mechanisms responsible for sugar transport within plants are well known that sugars produced by photosynthesis are transported through the phloem to the sink tissues. The second hypothesis is based on the effect of environmental conditions on the composition and viscosity of phloem sap, which determines the rate of phloem flow and translocation of nutrients or photoassimilates (Van Bel and Hess 2008; Liu *et al.* 2012). In this context, it is known that if the sugar concentration is low, only small amounts of energy are transferred from the source to the sink tissues. On the contrary, if it is too high the viscosity of the phloem sap impedes the flow.

Effect of "escaping positrons"

In the last type of experiments, we focused on the phenomenon of "escaping positrons", which is related to the annihilation of positrons outside plant tissues as very thin structures. This negative effect in the case of plant structures and organs (especially leaves) significantly affects the qualitative and quantitative aspects of PET analysis of the uptake, transport and distribution of radioindicators in living plants. The mentioned phenomenon was previously studied and described by some authors through the covering the analyzed plant object with different types of plastics or metal foils. Alexoff *et al.* (2011) measured the magnitude and distribution of escaping positrons from the leaf of tobacco (*N. tabacum* L.) for the radionuclides ^{18}F, ^{11}C and ^{13}N using a commercial small-animal PET scanner. They were used a thin plate of plexiglass to prevent the escape positrons and the annihilation of positrons outside the studied object.

In the Fig. 4 can be seen the distribution of 2-[^{18}F]FDG after 30 min of exposure of tobacco (*N. tabacum* L.) leaf immersed with excised leaf tip into a 2-[^{18}F]FDG solution containing 0.00762 mg.mL^{-1} D-glucose and initial ^{18}F

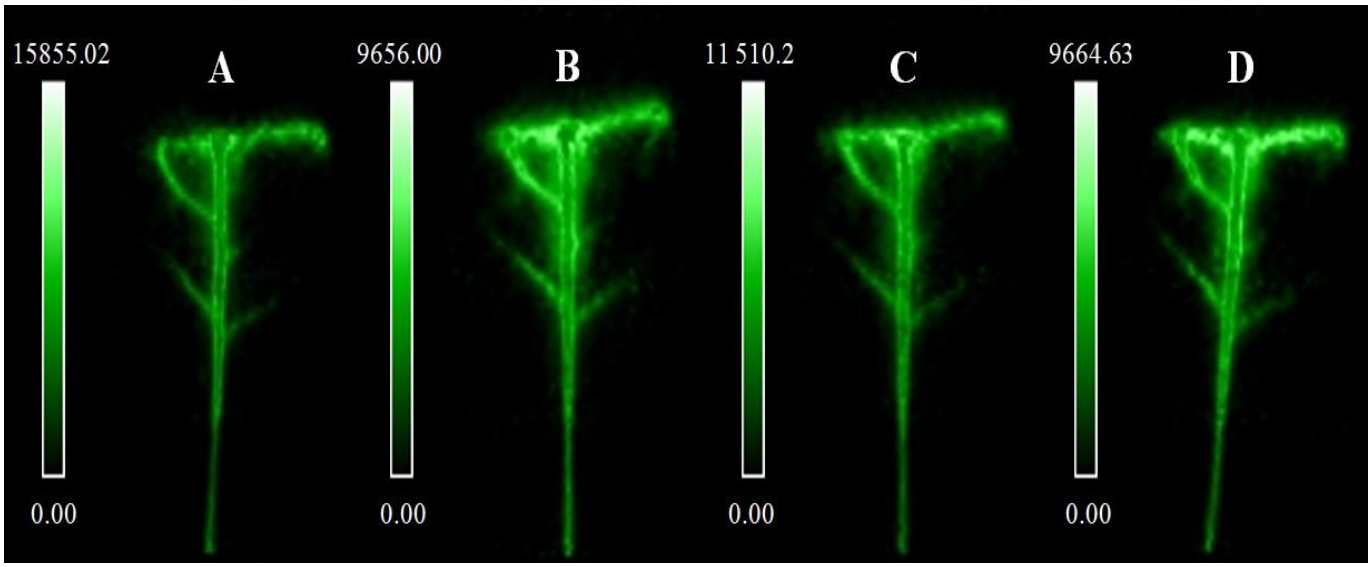

Fig. 4. Imaging of 2-[^{18}F]FDG distribution in the tissues of tobacco (*N. tabacum* L.) leaf immersed with the excised apex of the leaf blade into a 2-[^{18}F]FDG solution (A_0 = 40 MBq; c_{glu} = 0.00762 mg.mL^{-1}). After 30 min of exposure leaf was analyzed by a commercial microPET system with the acquisition time 2 min for bed position and under conditions: (**A**) uncovered leaf; (**B**) leaf covered by a parafilm; (**C**) leaf covered by an aluminium foil of thickness 0.1 mm; or (**D**) leaf covered by a copper plate of thickness 0.5 mm. The maximum threshold *TH* (thresholding-based methods) was reduced to 10%.

Table 3. Obtained quantitative data (variables) from the PET analysis of tobacco (*N. tabacum* L.) leaf under conditions: uncovered leaf (Leaf A); leaf covered by a parafilm (Leaf B); leaf covered by an aluminium foil of thickness 0.1 mm (Leaf C); or leaf covered by a copper plate of thickness 0.5 mm (Leaf D). For details, see Fig. 4.

Parameter/Variable	Leaf A	Leaf B	Leaf C	Leaf D
EV [cm^3]	2.027	3.314	2.478	3.061
PV	17,415	28,480	21,291	26,307
TGV	5 659,020	6 931,595	6 167,039	7 321,765
Mean TGV/EV	2 792,370	1 831,720	2 020,860	1 800,080
Mean TGV/PV	325.0	213.2	235.2	209.5
Max PV	15,855	9,656	11,510	9,665
EA [MBq]	1.043	1.269	1.134	1.339

EV – estimated volume within the PET analysis; *PV* – pixel volume; *TGV* – total gray value; *Mean TGV/EV* – mean total gray value divided by estimated volume of the leaf; *Mean TGV/PV* – mean total gray value divided by pixel volume of the leaf; *MaxPV* – maximum pixel value; *EA* – estimated ^{18}F activity accumulated in the leaf within the PET analysis.

activity A_0 = 40 MBq. Thus, the transport of photoassimilates in the basipetal way in this experiment was studied. After the primary PET analysis of tobacco leaf without covering (A), this leaf was subsequently covered with a parafilm (B), aluminium foil (C; thickness 0.1 mm) or copper thin plate (D; thickness 0.5 mm).

Based on the obtained 3D PET images (Fig. 4), it can be claimed that visually there were no significant changes in imaging the distribution of 2-[^{18}F]FDG in tobacco leaf tissues. However, quantitative data obtained from the PET analysis indicate significant changes in the values of the defined variables. In the Table 3, it can be seen that in the case of covering the leaf with a parafilm or copper plate, higher values were obtained for the parameters or variables, such as estimated volume of the visualized leaf (*EV*), pixel volume (*PV*), as well as the total gray value (*TGV*) and estimated activity of 2-[^{18}F]FDG according to the linear regression equation *TGV vs. VA* (volume activity of ^{18}F) compared to uncovered leaf. On the other hand, a significantly lower value of maximum pixel value (*Max PV*) was found, which defines the maximum value of pixel intensities in the entire 3D image of the object.

These changes in the values of the analyzed parameters or variables can be explained

by the principle that the covering materials – parafilm or copper thin plate used to cover the tobacco leaf showed the ability to absorb part of the "escaping positrons" as well as γ-photons released during the annihilation process, which could result in reduced radioactive hot spots in the leaf blade. This fact is also confirmed by the lower values of *Max PV* estimated for these cases.

In this context, it must be added that lower values of *Max PV* can lead in the reconstruction of 3D PET images to obtain richer quantitative information in the form of higher *TGV* values (also in relation to *EA*) due to the fact that sites with lower pixel intensities within the studied object were not excluded to such an extent as in the case of wider ranges of pixel intensities (higher values of *Max PV*). These facts can also result in higher values of *EV* and *PV* as well.

Conclusions

In the last two decades, PET has undergone significant development, aimed primarily to increase the spatial resolution of scanned objects, thus not only improving the existing application capabilities, but enhancing its advantages in terms of obtaining quantitative results. An interesting fact is that the development of this modern imaging technique was to a significant extent also related to the studied objects belonging to research in the field of plant biology. Thus, while following specific methodological approaches, PET is included in the group of quantitative nuclear analytical methods. Due to the size and shape of plant objects compared to conventional PET objects, obtaining quantitative analytical results in the study of plants encounters difficulties resulting from thin structures of plant tissues.

Our results showed that commercial PET systems, developed primarily for small laboratory animals, can also be used for the non-invasive 3D imaging and quantitative evaluation of *in vivo* radiotracers dynamics in plants with sizable organs or structures (in micrometres; e.g. leaves) which are below the limits of the spatial resolution of these imaging systems. We also found that in order to obtain relevant results in plant research focused on plant production or on the study of the accumulation of toxic organic substances (e.g. pesticides) or toxic metals, it will be necessary to take into account various factors influencing PET analysis. As our results showed, these factors include the characteristics of the studied plant tissues and the processes taking place in them, the chemical characteristics of the applied radioindicator solution – the chemical concentration of the carrier as well as the phenomenon of "escaping positrons" occurring in plants as thin objects.

Acknowledgement

This work was supported by the Slovak Research and Development Agency under the contract No. APVV-15-0098.

Conflict of Interest

The authors declare that they have no conflict of interest.

References

Alexoff, DL, SDewey SL, Vaska P, Krishnamoorthy S, Ferrieri R Schueller M Schlyer DJ, Fowler JS (2011) PET imaging of thin objects: measuring the effects of positron range and partial-volume averaging in the leaf of *Nicotiana tabacum*. Nucl. Med. Biol. 38: 191-200.

Berg E, Cherry SR (2018) Innovations in Instrumentation for Positron Emission Tomography. Semin. Nucl. Med. 48: 311-331.

Fatangare A, Svatoš A (2016) Applications of 2-deoxy-2-fluoro-D-glucose (FDG) in plant imaging: Past, present, and future. Front. Plant Sci. 7: 483.

Ferrieri AP, Appel H, Ferrieri RA, Schultz JC (2012) Novel application of 2-[^{18}F]fluoro-2-deoxy-D-glucose to study plant defenses. Nucl. Med. Biol. 39: 1152-1160.

Hattori E, Uchida H, Harada N, Ohta M, Tsukada H, Hara Y, Suzuki T (2008) Incorporation and translocation of 2-deoxy-2-[^{18}F]fluoro-D-glucose in *Sorghum bicolour (L.)* Moench monitored using a planar positron imaging system. Planta 227: 1181-1186.

Hoagland DR (1920) Optimum nutrient solution for plants. Science 52: 562-564.

Hubeau M, Steppe K (2015) Plant-PET scans: *In vivo* mapping of xylem and phloem functioning. Trends Plant Sci. 20: 676-685.

Karve AA, Alexoff D, Kim D, Schueller MJ, Ferrieri RA, Babst BA (2015) *In vivo* quantitative imaging of photoassimilate transport dynamics and allocation in large plants using a commercial positron emission tomography (PET) scanner. Plant Biol. 15: 273.

Kurita K, Miyoshi Y, Nagao Y, Yamaguchi M, Suzui N, Yin Y-G, Ishii S, Kawachi N, Hidaka K, Yoshida E, Takyu S, Tashima H, Yamaya T (2020) Fruit PET: 3-D imaging of carbon distribution in fruit using OpenPET. Nucl. Instrum. Methods Phys. Res. 954: 161843.

Liu DD, Chao WM, Turgeon R (2012) Transport of sucrose, not hexose, in the phloem. J. Exp. Bot. 63: 4315-4320.

Moein MM, Nakao R, Amini N, Abdel-Rehim M, Schou M, Halldin C (2019) Sample preparation techniques for radiometabolite analysis of positron emission tomography radioligands; trends, progress, limitations and future prospects. Trends Anal. Chem. 110: 1-7.

Partelová D, Uhrovčík J, Lesný J, Horník M, Rajec P, Kováč P, Hostin S (2014) Application of positron emission tomography and 2-[^{18}F]fluoro-2-deoxy-D-glucose for visualization and quantification of solute transport in plant tissues. Chem. Pap. 68: 1463-1473.

Partelová D, Horník M, Lesný J, Rajec P, Kováč P, Hostin S (2016) Imaging and analysis of thin structures using positron emission tomography: thin phantoms and *in vivo* tobacco leaves study. Appl. Radiat. Isot. 115: 87-96.

Partelová D, Kuglerová K, Konotop Y, Horník M, Lesný J, Gubišová M, Gubiš J, Kováč P, Matušíková I (2017) Imaging of photoassimilates transport in plant tissues by positron emission tomography. Nova Biotechnol. Chim. 16: 32-41.

Suzui N, Tanoi K, Furukawa J, Kawachi N (2019) Recent advances in radioisotope imaging technology for plant science research in Japan. Quantum Beam Sci. 3: 18.

Thorpe CL, Williams HA, Boothman CH, Lloyd JR, Morri K (2019) Positron emission tomography to visualise *in-situ* microbial metabolism in natural sediments. Appl. Radiat. Isot. 144: 104-110.

Tran TM, Hampton CS, Brossard TW, Harmata M, Robertson JD, Jurisson SS, Braun DM (2017) *In vivo* transport of three radioactive [^{18}F]-fluorinated deoxysucrose analogs by the maize sucrose transporter ZmSUT1. Plant Physiol. Biochem. 115: 1-11.

Tsuji A, Uchida H, Yamashita T, Matsuhashi S, Ito T, Mizuniwa C, Ishioka NS, Watanabe S, Sekine T (2002) Uptake of ^{18}FDG and $^{13}NO^-$ in tomato plants. *In:* Saidoh M, Toraishi A, Namba H, Itoh H, Tanaka S, Naramoto H, et al. (eds.), TIARA Annual Report 35: 103-104.

Van Bel AJE, Hess PH (2008) Hexoses as phloem transport sugars: the end of a dogma? J. Exp. Bot. 59: 261-272.

Wang Q, Mathews AJ, Li K, Wen J, Komarov S, O`Sullivan JA, Tai, Y-C (2014) A dedicated high-resolution PET imager for plant sciences. Phys. Med. Biol. 59: 5613-5630.

Weisenberger AG, Kross B, Lee SJ, McKisson J, McKisson JE, Xi W, Zorn C, Howell CR, Crowell, AS, Reid CD, Smith M (2013) Nuclear physics detector technology applied to plant biology research. Nucl. Instrum. Methods Phys. Res. 718: 157-159.